Advances in Water Resources 33 (2010) 1176–1186

Contents lists available at ScienceDirect

Advances in Water Resources

journal homepage: www.elsevier.com/ locate/advwatres

Hydrologic drought prediction under climate change: Uncertainty modeling with Dempster–Shafer and Bayesian approaches

Deepashree Raje [a], P.P. Mujumdar [a,b,*]

[a] Department of Civil Engineering, Indian Institute of Science, Bangalore, Karnataka 560 012, India
[b] Divecha Center for Climate Change, Indian Institute of Science, Bangalore, Karnataka 560 012, India

ARTICLE INFO

Article history:
Received 27 February 2010
Received in revised form 2 August 2010
Accepted 3 August 2010
Available online 12 August 2010

Keywords:
Downscaling
Uncertainty
Drought
Dempster–Shafer
Bayesian
Streamflow

ABSTRACT

Representation and quantification of uncertainty in climate change impact studies are a difficult task. Several sources of uncertainty arise in studies of hydrologic impacts of climate change, such as those due to choice of general circulation models (GCMs), scenarios and downscaling methods. Recently, much work has focused on uncertainty quantification and modeling in regional climate change impacts. In this paper, an uncertainty modeling framework is evaluated, which uses a generalized uncertainty measure to combine GCM, scenario and downscaling uncertainties. The Dempster–Shafer (D–S) evidence theory is used for representing and combining uncertainty from various sources. A significant advantage of the D–S framework over the traditional probabilistic approach is that it allows for the allocation of a probability mass to sets or intervals, and can hence handle both aleatory or stochastic uncertainty, and epistemic or subjective uncertainty. This paper shows how the D–S theory can be used to represent beliefs in some hypotheses such as hydrologic drought or wet conditions, describe uncertainty and ignorance in the system, and give a quantitative measurement of belief and plausibility in results. The D–S approach has been used in this work for information synthesis using various evidence combination rules having different conflict modeling approaches. A case study is presented for hydrologic drought prediction using downscaled streamflow in the Mahanadi River at Hirakud in Orissa, India. Projections of *n* most likely monsoon streamflow sequences are obtained from a conditional random field (CRF) downscaling model, using an ensemble of three GCMs for three scenarios, which are converted to monsoon standardized streamflow index (SSFI-4) series. This range is used to specify the basic probability assignment (bpa) for a Dempster–Shafer structure, which represents uncertainty associated with each of the SSFI-4 classifications. These uncertainties are then combined across GCMs and scenarios using various evidence combination rules given by the D–S theory. A Bayesian approach is also presented for this case study, which models the uncertainty in projected frequencies of SSFI-4 classifications by deriving a posterior distribution for the frequency of each classification, using an ensemble of GCMs and scenarios. Results from the D–S and Bayesian approaches are compared, and relative merits of each approach are discussed. Both approaches show an increasing probability of extreme, severe and moderate droughts and decreasing probability of normal and wet conditions in Orissa as a result of climate change.

1. Introduction

Uncertainty in projected climate change arises from a number of sources [5]: (1) the formulation and accuracy of the General Circulation Model (GCM); (2) the magnitude of anthropogenic emissions; and (3) the temporal and spatial impacts of natural variations internal to the climate system. The first source of uncertainty, referred to as GCM uncertainty, can be attributed to the structural set-up (e.g. the choice of grid resolution and climate processes included), and variability in the internal parameterizations of a GCM. The second source of uncertainty, referred to as scenario uncertainty, arises due to uncertainty in evolution of socio-economic scenarios and human action. To account for the GCM and scenario uncertainties, the use of GCM and scenario ensembles is recommended for a realistic assessment of climate change impacts. Unlike the other sources of uncertainty, the third type of uncertainty resulting from the chaotic nature of the climate system is an inherent property of the real climate system. Some studies use ensembles of GCMs with different initial conditions for representing the impacts of this type of uncertainty. This uncertainty will always be present and cannot be reduced by human actions. The other sources of uncertainty are human caused, either by inadequate modeling or by uncertain understanding of how political and social processes turn out. Assessing regional hydrologic impacts of climate change through downscaling adds another source of uncertainty, through the choice

* Corresponding author. Department of Civil Engineering, Indian Institute of Science, Bangalore, Karnataka 560 012, India. Tel.: +91 80 2293 2669; fax: +91 80 2360 0290.
E-mail addresses: draje@civil.iisc.ernet.in (D. Raje), pradeep@civil.iisc.ernet.in (P.P. Mujumdar).

0309-1708/$ – see front matter © 2010 Elsevier Ltd. All rights reserved.
doi:10.1016/j.advwatres.2010.08.001

of downscaling method. These uncertainties, arising from 'incomplete' and 'unknowable' information [26], propagate through the climate change impact assessment in an inter-dependent, but not necessarily additive or multiplicative manner. Thus, cascading uncertainties up to the regional or local level leads to large uncertainty ranges at such scales [33,43]. It is necessary to apply rigorous methods for representing and quantifying uncertainty in order to assist a risk-based approach to decision-making.

Recent studies to quantify uncertainty in large-scale climate change prediction have typically used a comparison or spread of results from various GCMs, scenarios and downscaling methods, perturbation analysis of simplified climate models or expert opinion to quantify uncertainty in climate variables [16]. Uncertainty in predictions resulting from the GCMs is estimated by developing probability distributions of key parameters (such as climate sensitivity or strength of the terrestrial carbon sink), which are then propagated through the GCMs using a Monte Carlo method. Model structural uncertainty is usually assessed by generating and comparing results from multiple model formulations. Such uncertainty analysis results in a probability distribution for global or regional temperature increase corresponding to each emissions scenario. However, subjective judgments are often used for the choice of probability distributions for model parameters (e.g., [24]). Recently, Bayesian Monte Carlo updating approaches have been used to represent uncertainty in key model parameters [10,26,38,39]. Greene et al. [13] generated probabilistic regional temperature projections by using a multi-model ensemble of atmosphere–ocean GCMs, using a Bayesian linear model. A commonly used method of evaluating effects of climate change on flow regime is to use an ensemble of GCMs, scenarios and statistical downscaling/regional climate models to provide inputs to a hydrological model, and examine the range of effects on a statistic of the modeled hydrologic variables [1,3,24,29,44]. GCM and scenario uncertainties have been studied in terms of PDFs of a hydrologic drought indicator such as standardized precipitation index (SPI) [11], using an imprecise probability approach [12] and through a possibilistic approach for streamflow downscaling [25]. Prudhomme and Davies [28] examined uncertainties in climate change impact analyses on river flow regimes in the UK, using either a statistical or dynamical downscaling model for downscaling precipitation from an ensemble of GCMs and scenarios, propagated to river flow through a lumped hydrological model. They showed that uncertainties from downscaling techniques and emission scenarios are of similar magnitude, and generally smaller than GCM uncertainty. Kay et al. [17] compared sources of uncertainty with respect to impact on flood frequency in England. They considered six different sources of uncertainty: future greenhouse gas emissions; Global Climate Model (GCM) structure; downscaling from GCMs (including Regional Climate Model structure); hydrological model structure; hydrological model parameters and the internal variability of the climate system (sampled by applying different GCM initial conditions). Minville et al. [23] studied the impact of climate change on the hydrology of the Chute-du-Diable watershed in Canada by comparing the statistics on current and projected future discharge. They used ten equally weighted climate projections from a combination of five general circulation models (GCMs) and two greenhouse gas emission scenarios (GHGES) to define an uncertainty envelope of future hydrologic variables.

The present study evaluates the use of a generalized uncertainty measure using the Dempster–Shafer evidence theory, for quantifying uncertainty in regional climate change projections. An uncertainty modeling framework, which combines GCM, scenario and downscaling uncertainties is evaluated. The Dempster–Shafer (D–S) evidence theory, which can be considered a generalized Bayesian theory [6], is used for representing and combining uncertainty. The D–S theory has in recent years found wide applications in the fields of statistical inference, sensor fusion, expert systems, diagnostics, risk analysis, and decision analysis, due to its versatility in representing and combining different types of evidence obtained from multiple sources. In this work, the uncertainty combination methodology is applied to projections of hydrologic drought in terms of monsoon standardized streamflow index (SSFI-4) classifications, which are obtained from streamflow projections for the Mahanadi River at Hirakud in Orissa, India. Three GCMs (MIROC3.2, CGCM2 and GISS) with three scenarios each (A1B, A2 and B1) are used. A conditional random field (CRF) downscaling model [30] is used, whose output gives n-best predictions which are converted to SSFI-4 projections. These are then used to construct a Dempster–Shafer structure (DSS) through a basic probability assignment (bpa) on SSFI-4 classifications. Future projected DSSs of the hydrologic variable are combined using the Dempster–Shafer theory of evidence combination. Projections from GCMs are combined using Dempster's rule, Zhang's center combination rule and disjunctive consensus rule of combination to get the final projections for the hydrologic variable (SSFI-4 classifications) and the associated uncertainty. A Bayesian approach is also used to derive posterior distributions for frequencies of each SSFI-4 classification for the same case study from the ensemble projections of GCMs and scenarios. Caselton and Luo [4] presented a water resources example of an application of the Dempster–Shafer approach and compared results with those from a Bayesian scheme. Luo and Caselton [20] presented aspects of the D–S approach that contribute to its appeal when dealing with information sources on climate change through examples. Recently, Raje and Mujumdar [31] used the Dempster–Shafer theory for uncertainty modeling in development of a methodology to constrain uncertainty using a nonstationary downscaling relationship. The present study analyses the D–S approach in detail, and provides key insights into the applicability and advantages of the D–S theory in uncertainty representation and combination as compared to traditional uncertainty modeling approaches. A Bayesian approach is presented which combines GCM and scenario uncertainties to provide posterior distributions for each category of SSFI-4. Results from the D–S and Bayesian approaches are compared and contrasted in this paper, and the relative merits of each approach are discussed. It is seen that both approaches have several unique advantages, and could be used as complementary approaches in an uncertainty modeling framework for prediction of hydrologic impacts of climate change. The results from this work indicate an increasing probability of extreme, severe and moderate drought and decreasing probability of normal to wet conditions, as a result of decreasing monsoon streamflow in the Mahanadi River due to climate change.

The paper is organized as follows. Section 2 presents the uncertainty combination framework for hydrologic drought prediction using D–S theory. Section 3 presents the basis of the Bayesian approach used in this work. Section 4 presents a case study application of the methodologies to the Mahanadi River. Section 5 contains results and discussion. Section 6 presents concluding remarks and potential for future research.

2. Uncertainty modeling using Dempster–Shafer theory

2.1. Dempster–Shafer Theory

Risk analysts recognize two fundamentally distinct forms of uncertainty [14]: Type I uncertainty or aleatory uncertainty arising from environmental stochasticity, inhomogeneity of materials, fluctuations in time, variation in space or heterogeneity; and Type II or epistemic uncertainty which arises from scientific ignorance, measurement uncertainty, or other lack of knowledge. In the climate modeling and regional impact assessment problem, for example, Type I uncertainty typically arises from natural variability internal to the climate system, whereas GCM and scenario uncertainties can be classified as Type II uncertainty. Although probability theory is traditionally used to characterize both types of uncertainty, critics [35,41] claim that traditional probability theory using the frequentist approach may not be capable of capturing epistemic uncertainty. Bayesian probability applies traditional probabilistic methods to

epistemic or subjective uncertainty. However, Walley [41] argued that a theory embracing imprecise probabilities would be needed for this purpose. Shafer [35] argued that an approach that takes account of the indistinguishability of underlying states within bodies of evidence would be required. There are three major frameworks for the interval-based representation of uncertainty: imprecise probabilities [19,41]; possibility theory [7,46]; and the Dempster–Shafer (D–S) theory of evidence [6,35,36,45].

The Dempster–Shafer (D–S) theory [35] or the theory of belief functions is a mathematical theory of evidence which can be interpreted as a generalization of probability theory in which the elements of the sample space to which nonzero probability mass is attributed are not single points but sets [18]. The sets that get nonzero mass are called focal elements. The sum of these probability masses is one, however, the basic difference between D–S theory and traditional probability theory is that the focal elements of a Dempster–Shafer structure may overlap one another. The D–S theory also provides methods to represent and combine weights of evidence. A detailed description of terminology and definitions used in D–S theory is provided in Raje and Mujumdar [31], and this work only provides a brief overview of the terminology.

The Dempster–Shafer theory represents a problem domain by a set, Θ, of mutually exclusive and exhaustive atomic hypotheses called the Frame of Discernment. A function $\mathbf{m}$: $2^{\Theta} \rightarrow [0,1]$ is called a basic probability assignment (bpa) over Θ if it satisfies $\mathbf{m}(\phi) = 0$ and

$$\sum_{S \subseteq \Theta} m(S) = 1 \tag{1}$$

From the basic probability assignment, the upper and lower bounds of an interval can be defined. This interval contains the precise probability of a set of interest (in the classical sense) and is bounded by two nonadditive continuous measures called Belief (**Bel**) and Plausibility (**Pl**). The lower bound for a set A, **Bel**(A) is defined as the sum of all the basic probability assignments of the proper subsets (B) of the set of interest (A) ($B \subseteq A$). Formally, for all sets A that are elements of the power set, $A \in 2^{\Theta}$

$$\mathbf{Bel}(A) = \sum_{B \subseteq A} \mathbf{m}(B) \tag{2}$$

A function, **Pl**: $2^{\Theta} \rightarrow [0,1]$ is called a plausibility function satisfying

$$\mathbf{Pl}(A) = \sum_{B \cap A \neq \phi} \mathbf{m}(B) \tag{3}$$

The plausibility represents the upper bound for a set A, and is the sum of all the basic probability assignments of the sets (B) that intersect the set of interest (A) ($B \cap A \neq \phi$). The precise probability $P(A)$ of an event (in the classical sense) lies within the lower and upper bounds of Belief and Plausibility, respectively:

$$\mathbf{Bel}(A) \leq P(A) \leq \mathbf{Pl}(A) \tag{4}$$

2.2. Combination of evidence in D–S theory

Combination rules are aggregation methods for data obtained from multiple sources providing different assessments for the same frame of discernment. Appendix A gives formulations for each of the rules used in this work for combination of evidence. The original combination rule of multiple basic probability assignments known as the Dempster rule is a generalization of Bayes' rule [6]. This rule emphasizes the agreement between multiple sources and ignores all the conflicting evidence through a normalization factor. Weighted Dempster–Shafer allows taking into account the different reliabilities of the sources. The formulation of Zhang's Center Combination rule [47] uses a measure of the intersection of two sets. The Disjunctive Consensus rule [8] considers the union of the basic probability assignments, which does not reject any of the information asserted by the sources. The Mixing or p-averaging combination rule is a generalization of averaging for probability distributions [34].

2.3. Uncertainty modeling framework

The framework developed in this work for uncertainty modeling uses the Dempster–Shafer evidence theory. The steps involved in the methodology are as given below:

- Outputs from an ensemble of GCMs for various scenarios are used for downscaling monsoon streamflow using a conditional random field (CRF) downscaling model [30].
- The output range of n-best streamflow sequences are converted to hydrologic drought projections through monsoon standardized streamflow index (SSFI-4).
- The range of SSFI-4 projections is then used to construct a Dempster–Shafer structure (DSS) through a basic probability assignment (bpa) on SSFI-4 classifications.
- Future projected DSSs of the hydrologic variable are combined using the Dempster–Shafer theory of evidence combination.
- Projections across scenarios are first combined using the mixing combination rule.
- Projections from GCMs are subsequently combined using Dempster's rule, Zhang's center combination rule and disjunctive consensus rule of combination (Appendix A) to get the final projections for the hydrologic variable (SSFI-4 classifications) and the associated uncertainty.

Thus, the methodology combines downscaling uncertainty resulting from n-best projections, scenario uncertainty resulting from an ensemble of scenarios and GCM uncertainty resulting from an ensemble of GCMs. The following sections explain the steps involved in the methodology.

2.3.1. Downscaling monsoon streamflow

Conditional random fields (CRFs) have been introduced by Raje and Mujumdar [30] for downscaling daily precipitation. In this work, the CRF-downscaling model is used for downscaling monsoon monthly streamflow. Hence, the conditional distribution of the streamflow sequence at a site, given the monthly atmospheric (large-scale) variable sequence, is represented as a linear-chain CRF. Let the monthly streamflow sequence at a site be represented by $\mathbf{y}$, and the observed daily atmospheric variable sequence by $\mathbf{x}$. The conditional distribution of the streamflow sequence $\mathbf{y}$ is given as:

$$p(\mathbf{y}|\mathbf{x}) = \frac{1}{Z(\mathbf{x})} \exp\left\{ \sum_{t=1}^{T} \sum_{k=1}^{K} \lambda_k f_k\left(y_t, y_{t-1}, \mathbf{x}\right) \right\} \tag{5}$$

where $Z(\mathbf{x}) = \sum_{y} \exp\left\{ \sum_{t=1}^{T} \sum_{k=1}^{K} \lambda_k f_k(y, y', \mathbf{x}) \right\}$ is an instance-specific normalization function summed over all possible output sequences $\mathbf{y} = \langle y_1, y_2, \ldots y_T \rangle$, $\Lambda = \{\lambda_k\} \in \Re^K$ is a parameter vector, and $\{f_k(y, y', \mathbf{x})\}_{k=1}^{K}$ is a set of real valued feature functions defined on pairs of consecutive streamflow values and the entire sequence of atmospheric data. Various feature functions used in this model are: intercept and transition features, raw observation features, difference features and threshold features [31].

The model is trained using maximization of log-likelihood [37]. Prediction for a future scenario is made using the n-best Viterbi algorithm to compute the n most likely streamflow sequences. Details of the training and prediction methodology are provided in Raje and Mujumdar [31]. In order to keep n consistent across predictions for all GCMs and scenarios, n is chosen such that

$$\sum_{i=1}^{n} \ln(P_i) > -1000 \quad \text{i.e.} \quad \ln(P_1 P_2 \ldots P_n) > -1000 \tag{6}$$

where P_i is the probability of the ith most likely streamflow sequence. n computed in this way will be large if the probability of first few most

likely sequences does not decay quickly. Hence, for projections with high downscaling uncertainty, a large n value will result from Eq. (6), leading to a larger spread in results and vice versa. The spread of the projected CDFs is a measure of the uncertainty in streamflow projection due to downscaling, which can be attributed to uncertainty in the local system's response to large-scale atmospheric forcing.

2.3.2. Hydrologic drought projections

Standardized streamflow index (SSFI) is statistically similar to the standardized precipitation index (SPI) introduced by McKee et al. [21] for meteorological drought analysis. The SPI is a z-score, or the number of standard deviations that the observed value would deviate from the long-term mean, for a normally distributed random variable. The SPI is computed for several time scales, ranging from one month to 24 months, to capture the various scales of both short-term and long-term drought.

The methodology for computing SSFI is as follows. Since monsoon SSFI-4 is computed, the observed time series comprising of streamflow for monsoon months (Jun–Sept) for a sufficiently long period (1959–2005) is taken. This is converted to a 4-monthly aggregated streamflow time series. Then, an equi-probability transformation of the aggregated streamflow into a standard normal variable is performed. In this work, a gamma distribution was fitted to the monsoon four-monthly aggregated streamflow, which could be considered as annual streamflow (due to small non-monsoon contribution). Many studies have examined choice of a suitable distribution function in relation to annual streamflows. McMahon et al. [22] found that for Europe and portions of North America the normal pdf is often adequate but the 2-parameter lognormal and gamma were more generally applicable. Among these, the gamma pdf was shown to fit the annual streamflows better than a lognormal pdf for the 1221 rivers studied. This result is consistent with other recent studies using large datasets from very heterogeneous regions [40]. For computing the SSFI-4 for any future projected aggregated streamflow time series, the non-exceedence probability related to such aggregated values is calculated and the corresponding standard normal quantile is defined as the SSFI. Since representation and combination of uncertainty using the D–S framework requires the problem domain defined as mutually exclusive hypotheses, it is much more relevant to have SSFI classifications as hypotheses rather than arbitrarily defined monthly streamflow ranges. Drought classification based on SSFI values is shown in Table 1.

2.3.3. Converting to a Dempster–Shafer structure

Each scenario-GCM gives a projected range of CDFs for SSFI-4 classifications as n-best projections. This range is converted to an equivalent Dempster–Shafer structure (DSS). The frame of discernment for the problem domain used here is based on SSFI-4 classifications as $\Theta = \{$extreme drought, severe drought, moderate drought, normal, moderate wet, very wet, and extreme wet$\}$. In this work, the following methodology is used to construct a DSS, following Ferson et al. [9]. By extracting minimum and maximum predicted probabilities for each SSFI-4 classification, the left and right bounds of a probability box are constructed. These are step functions from zero to one with the horizontal axis being SSFI-4 classifications. Then a series of horizontal lines is drawn, one from each corner of the step function to the other bound. This process describes a collection of rectangles of various sizes and locations. The location of a rectangle along the horizontal axis defines a focal element of the Dempster–Shafer structure. The height of each rectangle is the basic probability mass associated with that interval.

Table 1
Drought classification based on SSFI values.

Classification	SSFI value
Extreme wet	SSFI ≥ 2
Very wet	$1.5 \leq$ SSFI < 2
Moderate wet	$1 \leq$ SSFI < 1.5
Normal	$-1 <$ SSFI < 1
Moderate drought	$-1.5 <$ SSFI ≤ -1
Severe drought	$-2 <$ SSFI ≤ -1.5
Extreme drought	SSFI ≤ -2

2.3.4. Combining projections

Each scenario-GCM gives a projected range of future CDFs for SSFI-4 classifications. This projected range is used to construct a Dempster–Shafer structure (DSS) by the basic probability assignment (bpa) and quantification of beliefs on SSFI-4 classifications. The DSSs obtained from all scenarios for a particular GCM are first combined using the mixing combination rule by assigning equal weights to each scenario, to get the bpa for the DSS corresponding to their combination (Eq. (A9)). Application of this rule is equivalent to averaging applied to probability distributions. The bpa for the combination is used to derive the belief and plausibility for each proposition (SSFI-4 classification) from Eqs. (2) to (3) respectively. After this combination, a DSS is obtained for each GCM by combining uncertainty across scenarios. These DSSs for each GCM are further combined across GCMs to get the final range of uncertainty. For combining projections from different GCMs, three different rules viz. weighted Dempster's rule, weighted Zhang's Center Combination rule and weighted Disjunctive Consensus rule are used with equal weights for each GCM (Eqs. (A4), (A6) and (A9)). The belief and plausibility for each SSFI-4 classification are then obtained to represent the final uncertainty.

3. Bayesian approach to uncertainty modeling

Bayesian methods provide an elegant means of uncertainty modeling through a probabilistic representation of model parameter uncertainty. They are increasingly used in presenting probability distributions of future climate, and facilitate better decision-making [32,42]. As per the Bayesian viewpoint, uncertainty in the parameters of the statistical model is expressed by treating them as random variables. A prior probability distribution is specified for the parameters, based on expert judgement or beliefs. An uninformative prior such as the uniform distribution can be used if there is no prior knowledge of the distribution. The likelihood of the model is the conditional distribution of the data given the model parameters. If θ is the vector of model parameters, $p(\theta)$ is their prior distribution, and $p(x|\theta)$ is the likelihood for the data x, under assumptions formulated in the model, then by Bayes theorem, the posterior distribution of θ is given by

$$p(\theta|x) = \frac{p(x|\theta).p(\theta)}{\int_0^1 p(x|\theta).p(\theta)d\theta}. \quad (7)$$

The denominator in Eq. (7) is the normalizing constant of the posterior distribution of θ, or the marginal distribution $p(x)$. For most inferences, $p(x)$ does not have a closed form. If the kernel of the posterior density of θ can be recognized, then a direct computation of $p(x)$ can be avoided. For example, when the posterior distribution of a parameter belongs to the same family as the prior, such prior distributions are called conjugate prior distributions.

3.1. Analytical form for statistical model

The distributional assumptions for the data (likelihood) and prior distributions for the parameters used in this work are described in this section. The data used is the series of SSFI-4 classifications, obtained from the most likely streamflow projection of the CRF-downscaling model, for each GCM-scenario combination. This is a discrete data series, with classifications at each time being an element of the set

$\Theta = \{$extreme drought, severe drought, moderate drought, normal, moderate wet, very wet, and extreme wet$\}$. Let $X_{i,j,k}$ be the data for the kth SSFI-4 classification downscaled from GCM i and scenario j. The parameter of interest is taken to be the probability of the k^{th} SSFI-4 classification. The likelihood function of the data is then assumed to follow the discrete binomial distribution

$$X_{i,j,k} \sim B(1, \omega_k). \tag{8}$$

The assumption underlying Eq. (8) is that the probability of observing any particular classification such as moderate drought at a particular time is independent of prior observations. Hence, the statistical model for observing x_k "successes" or instances of a particular classification k, such as extreme drought, in N "trials" or periods, is given by

$$p(x|\omega_k) = \binom{N}{x_k} \omega_k^{x_k} (1-\omega_k)^{N-x_k} \tag{9}$$

where

$$x_1 + x_2 + .. + x_7 = N. \tag{10}$$

The prior distribution for each of the parameters is assumed to follow a beta distribution with parameters a and b equal to 1,

$$p(\omega_k; a, b) = \frac{\Gamma(a+b)}{\Gamma(a)\Gamma(b)} \omega_k^{a-1} (1-\omega_k)^{b-1} \text{ for } 0 \le \omega_k \le 1. \tag{11}$$

This is in fact an uninformative uniform distribution prior, which is a special case of the beta distribution with parameters $a = 1$ and $b = 1$.

Then the form for the unnormalized posterior from Eq. (7) is obtained as

$$p(\omega_k|x) \propto \omega_k^{a + x_k - 1} (1-\omega_k)^{b + N - x_k - 1} \tag{12}$$

whose kernel is also a beta distribution with parameters $a' = a + x_k - 1$ and $b' = b + N - x_k - 1$. Hence, the form of the posterior distribution of parameter ω_k is obtained as

$$p(\omega_k|x) = \frac{\Gamma(N+a+b)}{\Gamma(a+x_k)\Gamma(b+N-x_k)} \omega_k^{a + x_k - 1} (1-\omega_k)^{b + N - x_k - 1}. \tag{13}$$

The likelihood function in Eq. (9) is equivalent to assuming a multinomial likelihood function for the data, with parameters $(\omega_1, \omega_2, .. \omega_7)$; $\sum \omega_i = 1$. The multinomial likelihood could also have been used, with the Dirichlet distribution as conjugate prior. The posterior in that case would be a joint posterior over the parameters. However since we are interested in the marginal posterior of each ω_k rather than the joint posterior of the parameters $(\omega_1, \omega_2, .. \omega_7)$, the binomial likelihood representation in Eq. (9) will suffice and provide identical results. The posterior density obtained by combining projections from the three GCMs and three scenarios is then

$$p(\omega_k|x) = \prod_{i=1}^{3} \prod_{j=1}^{3} \frac{\Gamma\left(N_{i,j} + a + b\right)}{\Gamma\left(a + x_{i,j,k}\right)\Gamma\left(b + N_{i,j} - x_{i,j,k}\right)} \times \omega_k^{a + x_{i,j,k} - 1} (1-\omega_k)^{b + N_{i,j} - x_{i,j,k} - 1} \tag{14}$$

which is a beta distribution with parameters

$$a' = a + \sum_{i=1}^{3} \sum_{j=1}^{3} x_{i,j,k} \quad \text{and} \quad b' = b + \sum_{i=1}^{3} \sum_{j=1}^{3} N_{i,j} - x_{i,j,k}. \tag{15}$$

The following section gives details of the case study application.

4. Case study application

The uncertainty quantification methodology discussed in the previous sections is used for the prediction of future streamflow of Mahanadi River at Hirakud reservoir in Orissa, India. The Mahanadi basin lies in eastern India between 80°–30′E to 86°–50′E longitude and 19°–20′N to 23°–35′N latitude, and flows east to the Bay of Bengal. The location of Hirakud dam on the Mahanadi River (21.32°N, 83.45°E) is shown in Fig. 1. There is no major control structure upstream of the Hirakud reservoir and hence the inflow to the dam is considered as unregulated flow. The river has high streamflow during June to September due to monsoon rainfall, with insignificant contribution from the groundwater during this season. In the non-monsoon season, low rainfall results in low flow conditions. Hence, only monsoon streamflow is downscaled in this study.

Monsoon streamflow is linked broadly to rainfall and evaporation, although land use is also an important factor in the streamflow generation process. In the present study, land use pattern is assumed to remain unchanged in the future. Mujumdar and Ghosh [25] used 2 m surface air temperature, mean sea level pressure (MSLP), geopotential height at 500 hPa and surface specific humidity as predictor variables for their case study on the Mahanadi River. As per Raje and Mujumdar [31] and Mujumdar and Ghosh [25], the present study also considers 2 m surface air temperature, MSLP, geopotential height at 500 hPa and surface specific humidity as predictors for modeling streamflow in the monsoon season. These variables were found to be significantly correlated with monsoon streamflow in the case study region. The methodology used for downscaling monsoon streamflow follows Raje and Mujumdar [31] and

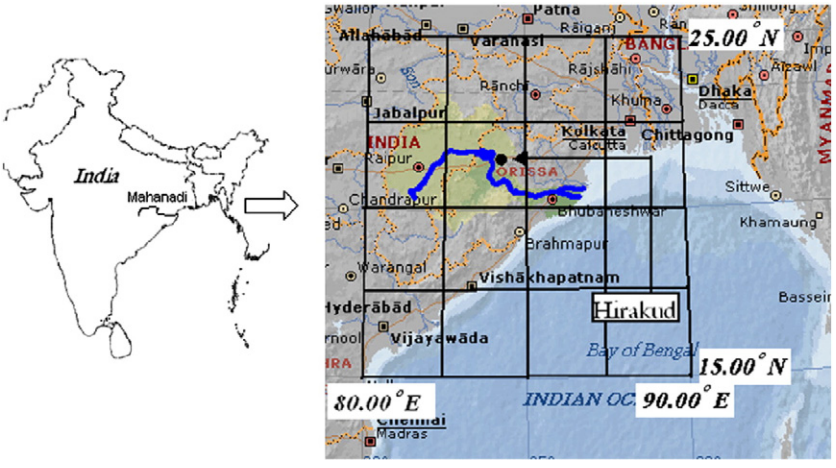

Fig. 1. Location of Hirakud dam on Mahanadi river (Source: Mujumdar and Ghosh, 2008).

Table 2
Training performance statistics for the CRF-downscaling model.

Streamflow statistics for training (1959–2005)		
	Observed	Computed
Mean (Mm^3)	7511.1	7456.1
Std deviation (Mm^3)	7012.5	6479.9
Skewness	2.2	1.2
Kurtosis	12.9	4.7

Table 3
Testing performance statistics for the CRF-downscaling model.

Streamflow statistics for testing (1990–2005)		
	Observed	Computed
Mean (Mm^3)	6870.8	6062.5
Std deviation (Mm^3)	6004.2	4797.1
Skewness	1.1	0.6
Kurtosis	4.0	2.5

includes bias removal and principal component analysis of the predictor variables, followed by a training of the CRF model.

Monsoon monthly mean inflow data for the Hirakud dam for years 1959–2005 is obtained from the Department of Irrigation, Government of Orissa, India. Predictor variable data is obtained from the National Center for Environmental Prediction/National Center for Atmospheric Research (NCEP/NCAR) reanalysis project for years 1948–2008 [15] for a region spanning 15°–25°N and 80°–90°E for years 1959–2005. For future monsoon streamflow projections, predictor variable data from the Intergovernmental Panel for Climate Change Assessment Report 4 (IPCC AR4) dataset for three GCMs for three scenarios each (A2, A1B, B1) is extracted for two time slices of years 2045–65 and 2075–95 from the multi-model dataset of the World Climate Research Programme's Coupled Model Intercomparison Project (WRCP CMIP3). For comparing GCM performance for the current climate, data for the 20C3M scenario (climate of the 20th century) for all GCMs for years 1960–2000 is also extracted. The GCMs used are CGCM2 (Meteorological Research Institute, Japan), MIROC3.2 (Center for Climate System Research, Japan) medium resolution version and GISS model E20/Russell (NASA Goddard Institute for Space Studies, USA), which are chosen based on availability of predictor variable data for all scenarios. The choice of time slices is made in order to represent conditions for a 'reasonably distant future' (2045–65) and a 'far distant future' (2075–95) and to project changes in uncertainty with time. Similarly, the choice of scenarios is made in order to represent extreme (high, A2 and low, B1) and medium (A1B) emissions trajectories.

Table 2 shows training performance statistics for the CRF-downscaling model. In order to validate the model, it is trained on a subset of the data for years 1959–1989, and tested on the remaining part for years 1990–2005. Table 3 shows the testing performance statistics for the case study site, obtained in independent testing for years 1990–2005.

The CRF-downscaling model is used for the projection of monsoon streamflow for the current period (years 1960–2000) and the future period (years 2045–65 and 2075–95). Fig. 2 shows the range of CDFs of projected monsoon monthly streamflow across three scenarios and three GCMs. Each GCM-scenario combination gives a band of *n*-best CDFs (many lines) for that combination, hence, there are three bands for each GCM (like three pink bands for CGCM2) in future projections. For years 1960–2000, only one scenario (20C3M) is used, so there is only one band for each GCM. It is seen that as the spread of projected CDFs increases, the farther we project into the future. Fig. 3 shows a gamma distribution fitted to the Hirakud 4-monthly aggregated monsoon streamflow data

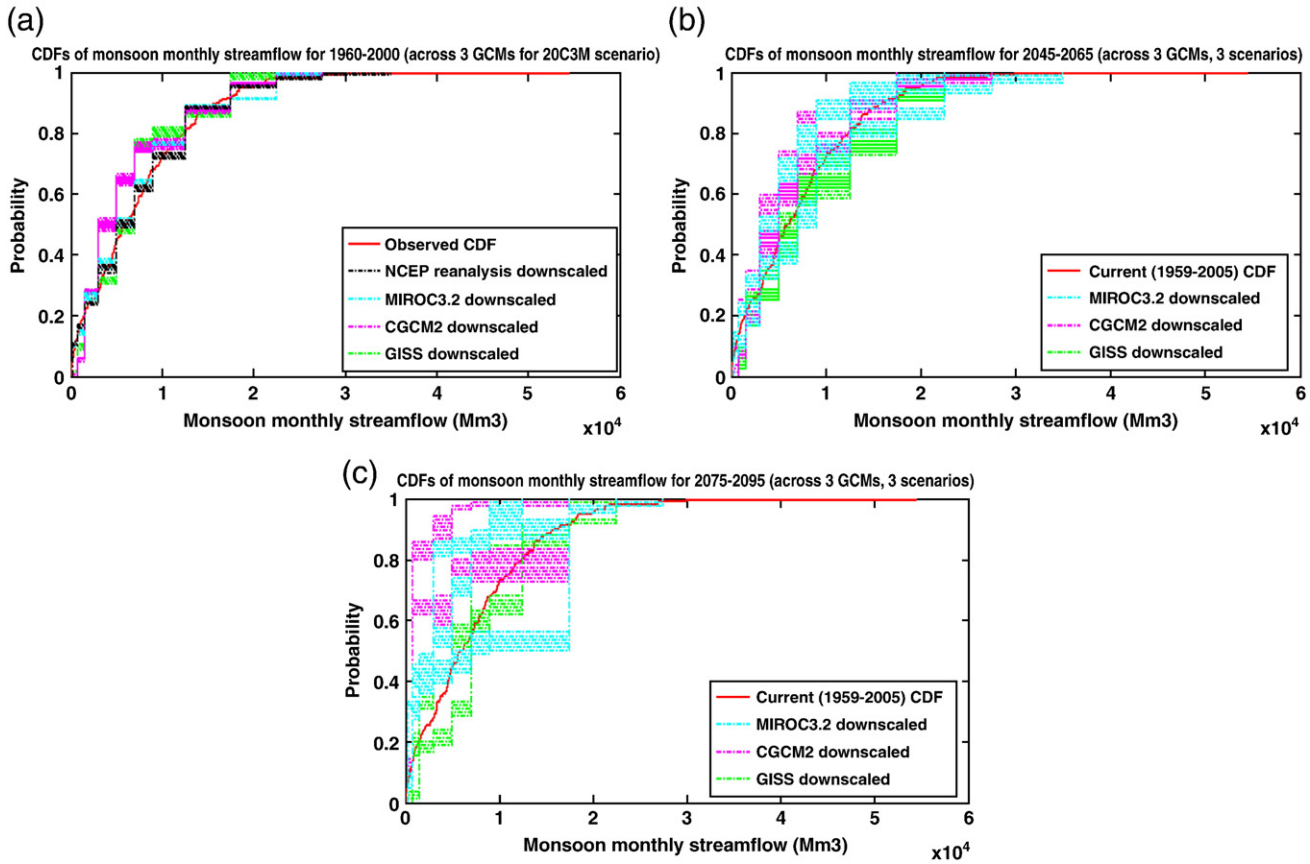

Fig. 2. Range of projected CDFs (a) across three GCMs for years 1960–2000 and (b) across three GCMs and three scenarios for years 2045–65 and (c) years 2075–95. Each GCM-scenario combination gives a 'band' of *n*-best CDFs for that combination.

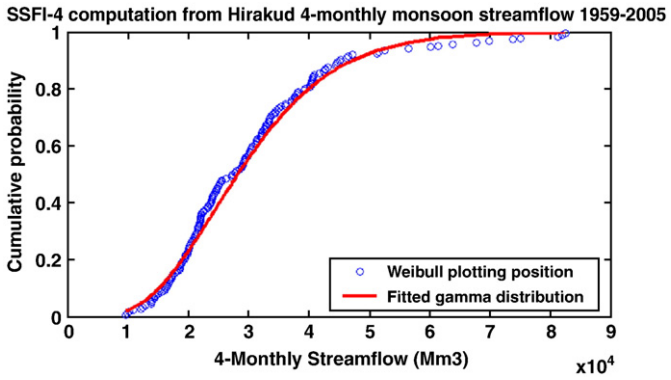

Fig. 3. Gamma distribution fitted to Hirakud 4-monthly monsoon streamflow for SSFI-4 computation (parameters $k = 5.48$, $\theta = 5488.1$ Mm^3, mean = 30074.7 Mm^3).

for years 1959–2005. It is seen that the gamma distribution provides a reasonably good fit to the data, however the upper tail of the distribution for higher streamflow values is not well matched. Fig. 4 shows the range of SSFI-4 classifications obtained for the current period (1960–2000) and a future period (years 2045–65). Again, each GCM-scenario combination gives a band of n-best CDFs for that combination, hence there are three bands of a given color in future projections.

It can be seen from Fig. 4(a) that the NCEP-downscaled projections match the observed CDF of SSFI-4 classifications well. This is because NCEP data is used for training the downscaling model. The three GCMs, on the other hand, show a bias in simulation of the current climate. None of the GCMs is able to reproduce the probabilities for very wet and extreme wet classifications satisfactorily. It can also be seen from Fig. 4(b) that there is an unacceptably large range of uncertainty in the probabilities of

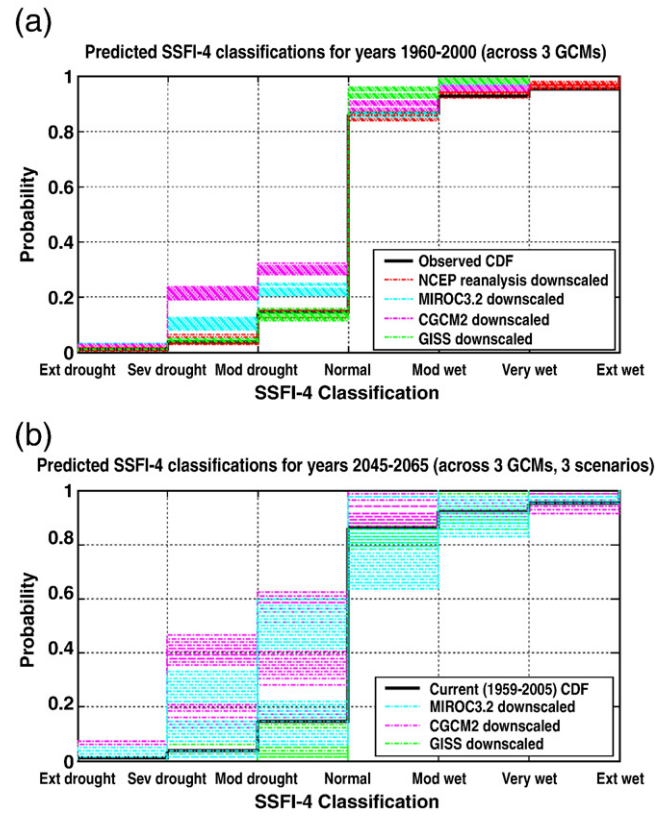

Fig. 4. Range of SSFI-4 classifications for current and future years (a) across 3 GCMs for years 1960–2000 (20C3M experiment) (b) across 3 GCMs, 3 scenarios for years 2045–65. The 'uncertainty envelope' enclosing the spread of projections across GCMs and scenario captures of GCM, scenario and downscaling uncertainties. Initial condition uncertainty is not included.

most SSFI-4 classifications if an 'uncertainty envelope' enclosing the spread across GCMs and scenarios is used for representing uncertainty.

5. Results and discussion

Fig. 5 shows the cumulative belief and plausibility functions after the combination across scenarios for years 2045–65, for all GCMs. The mixing combination rule is a generalization of averaging used for probability distributions (Eq. (A9)). Hence, Fig. 5 effectively represents mean cumulative probabilities (in a classical sense) for each SSFI-4 classification obtained by averaging regional projections for each GCM across different scenarios.

Fig. 6 shows the results after combining GCM uncertainty using the weighted Dempster's rule, weighted Zhang's Center Combination rule

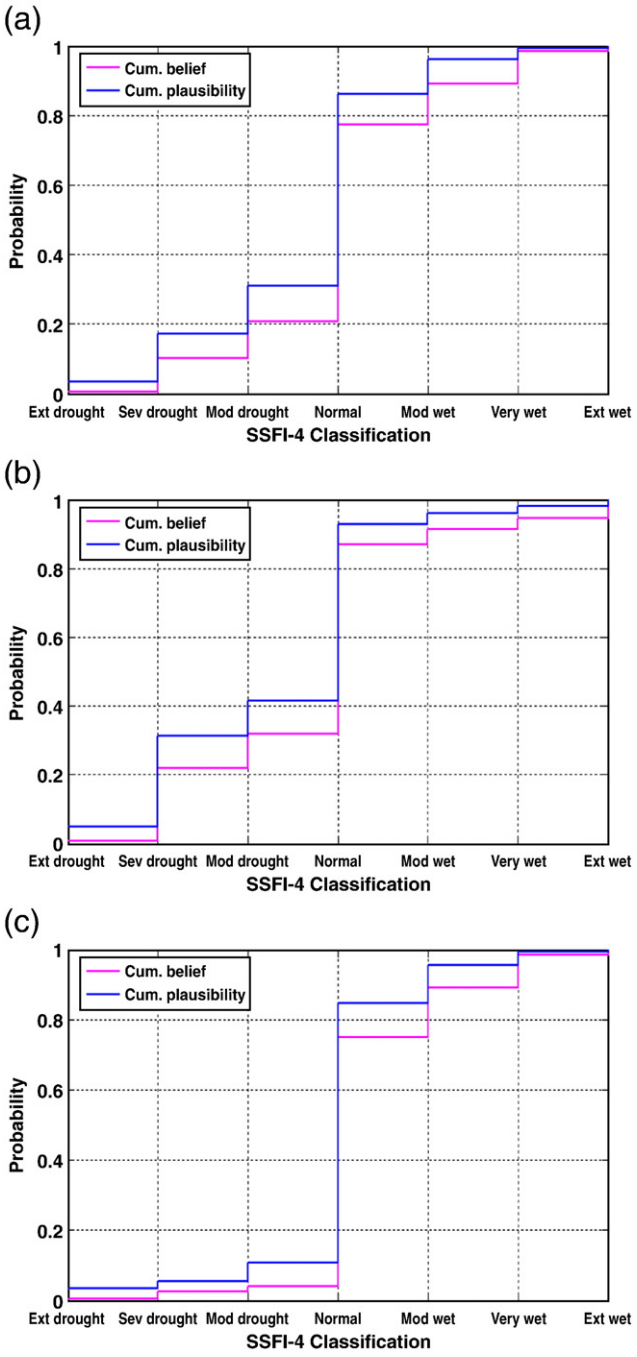

Fig. 5. Cumulative belief and plausibility functions for years 2045–65 for the GCMs: (a) MIROC3.2 (b) CGCM2 and (c) GISS.

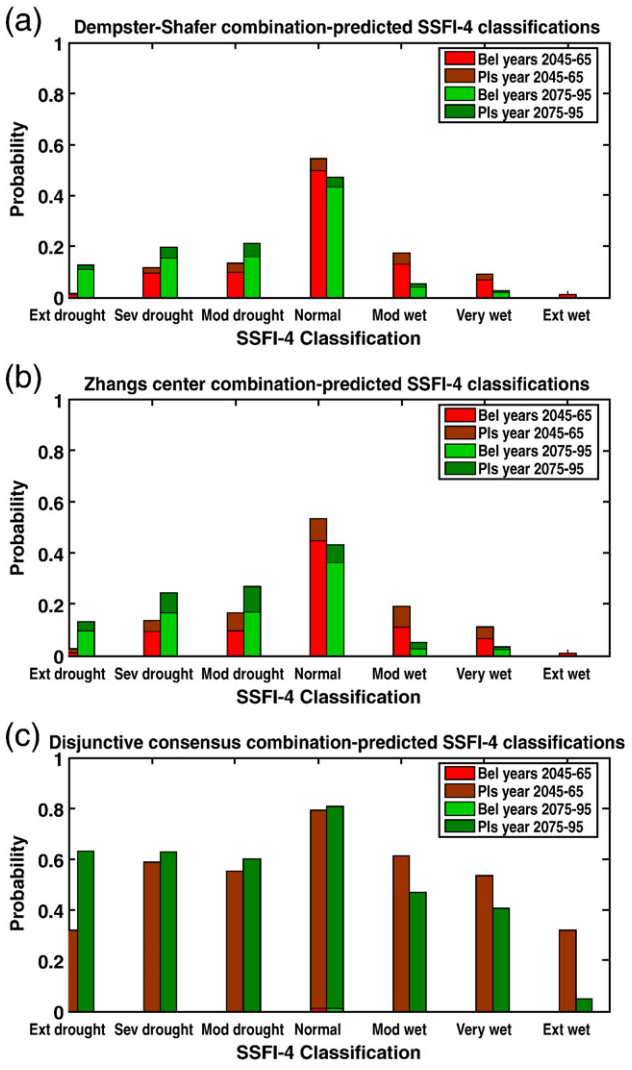

Fig. 6. Final combined uncertainty in terms of belief and plausibility for SSFI-4 classifications for years 2045–65 and 2075–95 using (a) Dempster's rule (b) Zhang's center combination rule and (c) Disjunctive consensus rule.

and weighted Disjunctive Consensus rule (Eqs. (A4), (A6) and (A8)) with equal weights assigned to GCMs. The difference between plausibility and belief for a given classification shows the associated uncertainty. Since Dempster's rule ignores all conflicting evidence, application of this rule yields the smallest band of uncertainty. Disjunctive Consensus based on the union operation does not ignore any evidence and hence shows the largest uncertainty. Since the Disjunctive Consensus rule is based on the union operation, there is a large uncertainty in the combination results, where the belief or lower bound on probability of an SSFI classification may be near zero. In other words, there is no probability mass which is confined to a singleton set (such as {severe drought}), but almost entirely, the probability mass is assigned to sets with cardinalities of two or more (such as {severe drought, moderate drought}). It is seen that there is an increasing probability of drought and decreasing probability of normal and wet conditions with time based on the SSFI-4 classifications.

Several factors have influenced the choice of a combination rule in this work. For combining scenario projections, the mixing rule is used, which is a generalization of averaging used for probability distributions. In this case, application of Dempster's rule which emphasizes agreement between sources or Disjunctive Consensus rule which does not reject any of the information asserted by the sources would have been inappropriate, because in combining scenario uncertainty, the aim is not to use a measure of agreement or disagreement between scenarios. Subsequently, in combination of GCM uncertainty, these rules explore the continuum between the 'AND' operation to the 'OR' operation. In combination of GCM uncertainty, essentially a projection using multiple information sources with varying performances is used. In the present work these reliabilities with respect to performance are taken as equal, but they could be based on some measure of performance to appropriately weight GCMs, such as the GCMs' ability to simulate streamflows for the 20th century. If the GCMs show largely conflicting evidence (predictions), then application of Dempster's rule for evidence combination may not be appropriate, since this rule attributes any probability mass associated with conflict to the null set [45]. In the case of conflicting projections, use of the Disjunctive Consensus rule may be more suitable, but this rule gives highly imprecise results with large uncertainty, which is impractical for application. Since most GCMs do not provide vastly conflicting predictions, the Dempster's rule might be sufficient to provide a realistic estimate of uncertainty.

The Bayesian modeling approach is used in this work to derive posterior distributions for the frequencies of each SSFI-4 classification using the statistical model outlined in Section 3. The expected value of the posterior distribution for each classification is compared to the belief and plausibility values for that classification obtained through the D–S analysis. Fig. 7 shows derived posterior distributions from the

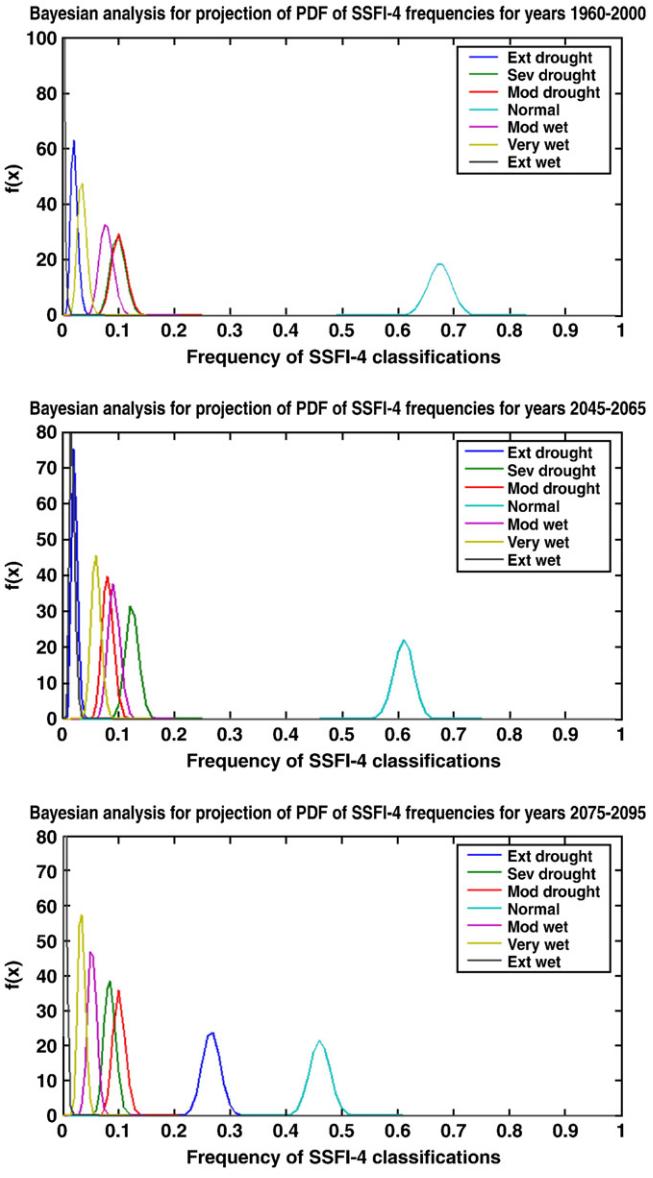

Fig. 7. Posterior distributions of SSFI-4 classifications obtained from Bayesian analysis.

Table 4
Statistics for posterior distributions of frequencies of SSFI-4 classifications.

SSFI-4 category	Mean freq.	Std dev. of freq.	Mean freq.	Std dev. of freq.	Mean freq.	Std dev. of freq.
Years	1960–2000		2045–65		2075–95	
Extreme drought	0.021	0.006	0.022	0.005	0.267	0.016
Severe drought	0.099	0.014	0.124	0.012	0.085	0.01
Moderate drought	0.101	0.014	0.081	0.01	0.101	0.011
Normal	0.674	0.021	0.61	0.018	0.461	0.018
Moderate wet	0.078	0.012	0.092	0.011	0.053	0.008
Very wet	0.035	0.008	0.06	0.009	0.034	0.007

Bayesian approach, for the present (1960–2000) 20C3M scenario, and for the future time slices 2045–65 and 2075–95.

The derived posterior distributions show aspects which are not evident from a single valued parameter estimate, such as the spread and tails of the distribution. The distributions show that the mean frequency of normal conditions decreases in the future, and that of drought conditions increases in future. Table 4 gives the mean and standard deviation values of posterior distribution of the parameters. Fig. 8 shows the current versus Bayesian-predicted expected values of SSFI-4 probabilities for the future. The trend from 1960–2000 to 2045–65 shows an increasing probability of drought and simultaneous increasing probability of wet conditions. The trend from 2045–65 to 2075–95 shows an increasing probability of drought and decreasing probability of wet conditions. Hence the trend appears to be insignificant for every category except normal and extreme drought, based on the inconsistent sign of the change in the other categories. Drying trends would be expected to be monotonic between mid and late century.

Fig. 9 presents a comparison of results obtained from the D–S approach and expected values from the Bayesian scheme. The Dempster's rule is used in obtaining results in the D–S approach. Both approaches show broad agreement in the direction of changes, but magnitudes of the projected changes in frequencies differ. The Bayesian approach used here provides a distribution of frequency for each category of SSFI-4, while the D–S approach provides an uncertainty range in terms of belief and plausibility. This is due to additional assumptions about the likelihood function made in the Bayesian approach. Also, the D–S approach includes downscaling uncertainty represented as overlapping bpas from *n*-best projections, while the Bayesian approach uses singleton probabilities from the most likely projection for each GCM-scenario combination.

This work does not implement the Bayesian approach in the same uncertainty modeling framework as the D–S analysis, since the objective of the work is to analyze how best each approach can be implemented in the climate change problem. The evidence combination using Dempster's rule of combination is analogous to Bayes' equation in the Bayesian scheme, and the resultant bpa is analogous to the Bayesian posterior distribution. D–S combination becomes Bayesian combination in the special case in which mass is assigned only to singleton sets. However, a bpa in general is not a Bayesian probability. The bpa $\mathbf{m}(A)$ is a level of confidence in exactly a specific hypothesis, A. It does not include the confidence in any particular subset of that hypothesis. Also, in contrast to Bayesian approaches, it does not imply the amount of probability assigned to its negation. The Bayesian approach replaces ignorance with indifference. The D–S theory has hence been claimed to be a generalized Bayesian theory [35]. Luo and Caselton [20] have earlier shown that the Bayesian approach has shortcomings under near-ignorance conditions, primarily due to the restriction placed on Bayesian probability assignments that they can only be made to mutually exclusive point values or intervals. When epistemic uncertainty is represented in the form of non-singleton overlapping bpas, the D–S combination has been shown to perform better than Bayesian combination in fields such as multi-sensor data fusion [2]. Even then, the upper and lower compatible distributions of the D–S analysis have been shown to converge to the Bayesian posterior with increasing number of data combinations [4]. When all the evidence assignments are non-Bayesian, replacement of the D–S computation with the corresponding Bayesian computation, results in loss of the uncertainty estimate, as uncertainty is distributed among all components of the composite mass. This likely will not be a significant drawback in situations when uncertainty is small, since the results of D–S and Bayesian evidence accumulations converge quickly. However, a loss of potentially useful information might possibly occur when uncertainty assumes an intermediate to high value, such as in climate change impacts assessment. This loss needs to be evaluated, and compared with the gains brought about by the replacement of the D–S approach with the Bayes approach, which is reduction of computational complexity of the combining operation and simplification of the analysis.

There are some assumptions and limitations of the D–S and Bayesian models presented in this work. The monsoon standardized streamflow index (SSFI-4) used here is assumed to be representative of drought and wet conditions since it depicts water supply availability. Orissa state

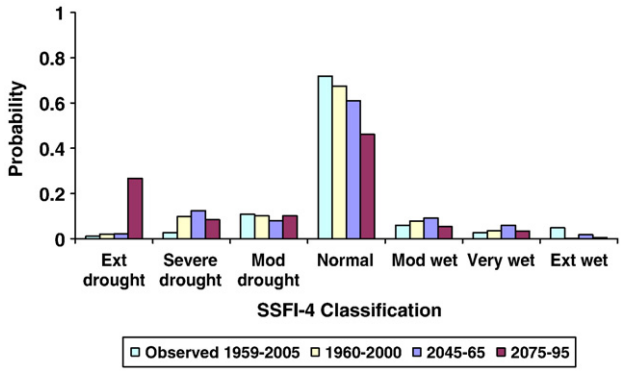

Fig. 8. Expected values of frequencies of SSFI-4 classifications obtained from posterior distributions of Bayesian analysis.

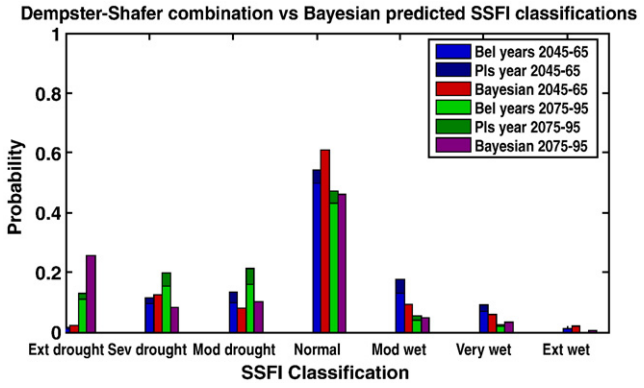

Fig. 9. Comparison of results from the Dempster–Shafer and Bayesian approaches for uncertainty modeling of SSFI-4 classifications.

receives about 116.7 cm of rainfall during the southwest monsoon season from June to September, which constitutes about 80% of the annual rainfall over Orissa [27]. However, if climate change results in a change in this pattern with more proportion of non-monsoon rainfall then the SSFI-4 would not provide a true representation of drought/wet conditions. Use of multiple downscaling models in this methodology would provide robustness in prediction. Weighted combination rules could be used to weight different GCMs and obtain a better final uncertainty estimate. The Bayesian statistical model assumes a binomial likelihood for the frequency of each category of drought. If likelihood function is assumed differently, say as Poisson distributed with a gamma prior, then the results obtained for the posterior and its expected value could be different. Hence, results from the analysis need to be interpreted appropriately.

6. Concluding remarks

Prediction at regional scales is subject to large uncertainties which must be quantified for informed decision-making. The results from this work indicate an increasing probability of extreme, severe and moderate drought in Orissa and decreasing probability of normal to wet conditions due to a decrease in monsoon streamflow in the Mahanadi River, as a result of climate change. The D–S approach presented combines GCM, scenario and downscaling uncertainties. Since the D–S evidence combination framework presented in the paper can handle epistemic as well as aleatory uncertainty, it is well suited to the climate change impact assessment problem. The D–S theory shows a relatively high degree of theoretical development among the nontraditional theories for characterizing uncertainty, but is related to traditional probability theory and set theory. It shows good versatility to represent and combine different types of evidence obtained from multiple sources. The Bayesian approach provides new insights into the distributions of parameters of the statistical model, and is hence an important tool in climate change uncertainty modeling. Both approaches show broad agreement in projections for regional impact assessment. Both D–S and Bayesian frameworks could be used as complementary approaches for quantifying uncertainty in regional impacts of climate change. Generalized uncertainty-based information theories can be explored in order to handle the various types of uncertainty presented in climate and hydrologic modeling problems, and their implications for policy needs to be studied.

Appendix A. Combination rules in Dempster–Shafer theory

A.1. Dempster's rule

Dempster's rule combines multiple belief functions through their basic probability assignments (**m**) as

$$m_{12}(A) = m_1 \oplus m_2(A) = \frac{\sum_{B\cap C=A} m_1(B)m_2(C)}{1-K} \text{ when } A\neq\phi \tag{A1}$$

$$m_{12}(\phi) = 0 \tag{A2}$$

where

$$K = \sum_{B\cap C=\phi} m_1(B)m_2(C). \tag{A3}$$

K represents basic probability mass associated with conflict, and indicates the degree of conflict between two distinct bodies of evidence. K is determined by summing the products of the bpas of all sets where the intersection is null. The denominator in Dempster's rule, 1-K, is a normalization factor. The effect of the denominator is that conflict is completely ignored and any probability mass associated with conflict is attributed to the null set [44]. Multiple sources can be combined sequentially using the above rule, the order of combination does not affect the final result.

A.2. Weighted Dempster's rule

Weighted Dempster–Shafer allows taking into account the different reliabilities of the sources. A high (low) weight is assigned to a more reliable (less reliable) source of evidence. For this, the weighted Dempster's rule can be used [45]:

$$m_{12}(A) = m_1 \oplus m_2(A) = \frac{\sum_{B\cap C=A} m_1(B)^{w_1} m_2(C)^{w_2}}{\sum_{B\cap C\neq\phi} m_1(B)^{w_1} m_2(C)^{w_2}} \tag{A4}$$

where w_i is the weight assigned to source with bpa m_i. When $w_1 = w_2 = 1$, this equation reduces to the basic Dempster's rule of combination.

A.3. Zhang's center combination rule

Zhang pointed out that Dempster's rule fails to consider how focal elements intersect [46]. To define an alternative rule of combination, a measure of the intersection of two sets B and C assuming finite sets is introduced. This is defined as the ratio of the cardinality of the intersection of two sets divided by the product of the cardinality of the individual sets, denoted by $r(B,C)$:

$$r(B,C) = \frac{|B\cap C|}{|B||C|} = \frac{|A|}{|B||C|} \tag{A5}$$

where $B\cap C = A$. The resulting combination rule scales the products of the basic probability assignments of the intersecting sets ($B\cap C = A$) by using a measure of intersection, $r(B,C)$. This is repeated for every intersecting pair that yields A. The scaled products of the masses for all pairs whose intersection equals A are summed and multiplied by a renormalization factor k. This renormalization factor provides that the sum of the basic assignments is one. A weighted version of Zhang's rule is:

$$m_{12}(A) = k \sum_{B\cap C=A} \left[\frac{|A|}{|B||C|} m_1(B)^{w_1} m_2(C)^{w_2}\right]. \tag{A6}$$

A.4. Disjunctive consensus rule

Dubois and Prade take a set-theoretic view of a body of evidence to form their disjunctive consensus rule [8]. They define the union of the basic probability assignments $m_1 \cup m_2$ (denoted by $m_\cup(A)$) by extending the set-theoretic union:

$$m_\cup(A) = \sum_{B\cup C=A} m_1(B)m_2(C). \tag{A7}$$

A weighted disjunctive consensus rule is:

$$m_\cup(A) = \sum_{B\cup C=A} m_1(B)^{w_1} m_2(C)^{w_2}. \tag{A8}$$

The union does not generate any conflict and does not reject any of the information asserted by the sources. Hence, no normalization procedure is required. The drawback of this method is that it may yield a more imprecise result than desirable.

A.5. Mixing combination rule

Mixing (or p-averaging) is a generalization of averaging for probability distributions [30]. In this work, this rule has been used for combining scenario uncertainty. Mixing generalizes the averaging

operation usually used for probability distributions. The formula for the mixing combination rule is:

$$m_{12\ldots n}(A) = m_1 \oplus m_2 \oplus \ldots m_n(A) = \frac{\sum_{i=1}^{n} w_i m_i(A)}{\sum_{i=1}^{n} w_i} \tag{A9}$$

where m_i's are the bpas for the belief structures being aggregated and the w_i's are weights assigned according to the reliability of the sources.

References

[1] Booij MJ, Huisjes M, Hoekstra AY. Uncertainty in climate change impacts on low flows. IAHS-AISH Publ 2006;308:401–6.
[2] Braun J. Sensor fusion: architectures, algorithms, and applications IV. Proceedings of SPIE, Vol. 4051. Orlando, FL: SPIE Society of Photo-Optical Instrumentation Engineering; 2000. p. 255–66.
[3] Buytaert W, Celleri R, Timbe L. Predicting climate change impacts on water resources in the tropical Andes: effects of GCM uncertainty. Geophys Res Lett 2009;36(7):L07406.
[4] Caselton WF, Luo W. Decision making with imprecise probabilities: Dempster–Shafer theory and application. Water Resour Res 1992;28(12):3071–83.
[5] Cubasch U, Meehl GA, Boer GJ, Stouffer RJ, Dix M, Noda A, Senior CA, Raper SCB, Yap KS. Projections of future climate change. In: Houghton JT, Ding Y, Griggs DJ, Noguer M, van der Linden P, Dai X, Maskell K, Johnson CI, editors. Climate Change 2001: the Scientific Basis. Contribution ofWorking Group I to the Third Assessment Report of the Intergovernmental Panel on Climate Change. Cambridge University Press; 2001. p. 525–82.
[6] Dempster AP. Upper and lower probabilities induced by a multivalued mapping. Ann Stat 1967;28:325–39.
[7] Dubois D, Prade H. Possibility Theory. New York: Plenum Press; 1988.
[8] Dubois D, Prade H. On the Combination of Evidence in Various Mathematical Frameworks, Reliability Data Collection and Analysis. Brussels: ECSC, EEC, EAFC; 1992. p. 213–41.
[9] Ferson S, Kreinovich V, Ginzburg L, Myers DS, Sentz K. Constructing probability boxes and Dempster–Shafer structures. Sandia National Laboratories 2002-0835; 2002.
[10] Forest CE, Stone PH, Sokolov AP, Allen MR, Webster MD. Quantifying uncertainties in climate system properties with the use of recent climate observations. Science 2002;295:113–7.
[11] Ghosh S, Mujumdar PP. Nonparametric methods for modeling GCM and scenario uncertainty in drought assessment. Water Resour Res 2007;43:W07405, doi:10.1029/2006WR005351.
[12] Ghosh S, Mujumdar PP. Climate change impact assessment: uncertainty modeling with imprecise probability. J Geophys Res 2009;114:D18113, doi:10.1029/2008JD011648.
[13] Greene AM, Goddard L, Lall U. Probabilistic multimodel regional temperature change projections. J Climate 2006;19(17):4326–43.
[14] Helton JC. Uncertainty and sensitivity analysis in the presence of stochastic and subjective uncertainty. J Stat Comput Simul 1997;57:3–76.
[15] Kalnay E, Kanamitsu M, Kistler R, Collins W, Deaven D, Gandin L, et al. The NCEP/NCAR 40-year reanalysis project. Bullet Amer Meteorol Soc 1996;77(3):437–71.
[16] Katz RW. Techniques for estimating uncertainty in climate change scenarios and impact studies. Climate Res 2002;20:167–85.
[17] Kay AL, Davies HN, Bell VA, Jones RG. Comparison of uncertainty sources for climate change impacts: flood frequency in England. Climate Change 2009;92(1–2):41–63.
[18] Klir G, Yuan B. Fuzzy Sets and Fuzzy Logic: Theory and Applications. New Jersey: Prentice Hall; 1995.
[19] Kuznetsov VP. Interval Statistical Models. Moscow: Radio i Svyaz Publ; 1991 (in Russian).
[20] Luo WB, Caselton B. Using Dempster–Shafer theory to represent climate change uncertainties. J Environ Manage 1997;49:73–93.
[21] McKee TB, Doesken NJ, Kleist J. The relationship of drought frequency and duration to time scale. Proceedings of the Eighth Conference on Applied Climatology. American Meteorological Society; 1993. p. 179–84.
[22] McMahon TA, Vogel RM, Peel MC, Pegram GS. Global streamflows—Part 1: characteristics of annual streamflows. J Hydrol 2007;347:243–59.
[23] Minville M, Brissette F, Leconte R. Uncertainty of the impact of climate change on the hydrology of a Nordic watershed. J Hydrol 2008;358:70–83.
[24] Morgan MG, Keith DW. Subjective judgments by climate experts. Environ Sci Technol 1995;29:468–79.
[25] Mujumdar PP, Ghosh S. Modeling GCM and scenario uncertainty using a possibilistic approach: application to the Mahanadi River India. Water Resour Res 2008;44:W06407, doi:10.1029/2007WR006137.
[26] New M, Hulme M. Representing uncertainty in climate change scenarios: a Monte Carlo approach. Int Assess 2000;1:203–13.
[27] Parthasarathy B, Munot AA, Kothawale DR. Monthly and Seasonal Rainfall Series for All India Homogeneous Regions and Meteorological Subdivisions:1871–1994. RR-065. Pune: Indian Institute of Tropical Meteorology; 1995.
[28] Prudhomme C, Davies H. Assessing uncertainties in climate change impacts analyses on the river flow regimes in the UK. Part 2: future climate. Clim Change 2009;93:197–222.
[29] Prudhomme C, Jakob D, Svensson C. Uncertainty and climate change impact on the flood regime of small UK catchments. J Hydrol 2003;277:1–23.
[30] Raje D, Mujumdar PP. A conditional random field based downscaling method for assessment of climate change impact on multisite daily precipitation in the Mahanadi basin. Water Resour Res 2009;45(10):W10404, doi:10.1029/2008WR007487.
[31] Raje D, Mujumdar PP. Constraining uncertainty in regional hydrologic impacts of climate change: nonstationarity in downscaling. Water Resour Res 2010;46:W07543, doi:10.1029/2009WR008425.
[32] Reilly J, Stone PH, Forest CE, Webster MD, Jacoby HD and RG Prinn, Uncertainty in Climate Change Assessments, Science 293 (5529), 430a., 2001: 430–433.
[33] Rowell DP. A demonstration of the uncertainty in projections of UK climate change resulting from regional model formulation. Clim Change 2006;79:243–57.
[34] Sentz K, Ferson S. Combination of evidence in Dempster–Shafer theory. Sandia National Laboratories 2002-4015; 2002.
[35] Shafer G. A Mathematical Theory of Evidence. Princeton: Princeton University Press; 1976.
[36] Smets P. The normative representation of quantified beliefs by belief functions. Artif Intell 1997;92:229–42.
[37] Sutton C, McCallum A. An introduction to conditional random fields for relational learning. Introduction to Statistical Relational Learning. Cambridge, MA: MIT Press; 2006. p. 1–35.
[38] Tebaldi C, Mearns LO, Nychka D, Smith RL. Regional probabilities of precipitation change: a Bayesian analysis of multimodel simulations. Geophys Res Lett 2004;31, doi:10.1029/2004GL021276.
[39] Tebaldi C, Smith R, Nychka D, Mearns LO. Quantifying uncertainty in projections of regional climate change: a Bayesian approach to the analysis of multi-model ensembles. J Climate 2005;18:1524–40.
[40] Vogel RM, Wilson I. Probability distribution of annual maximum mean and minimum streamflows in the United States. J Hydrol Eng 1996;1(2):69–76.
[41] Walley P. Statistical Reasoning with Imprecise Probabilities. London: Chapman and Hall; 1991.
[42] Webster M. Communicating climate change uncertainty to policy-makers and the public. Clim Change 2003;61:1–8.
[43] Wilby RL. Uncertainty in water resource model parameters used for climate change impact assessment. Hydrol Process 2005;19(16):3201–19.
[44] Wilby RL, Harris I. A framework for assessing uncertainties in climate change impacts: low-flow scenarios for the River Thames, UK. Water Resour Res 2006;42:W02419, doi:10.1029/2005WR004065.
[45] Yager RR. On the Dempster–Shafer framework and new combination rules. Inf Sci 1987;41:93–137.
[46] Zadeh LA. Fuzzy sets. Inf Control 1965;8:338–53.
[47] Zhang L. Representation, independence, and combination of evidence in the Dempster–Shafer theory. Advances in the Dempster–Shafer Theory of Evidence. New York: John Wiley & Sons, Inc; 1994. p. 51–69.